Hindawi
Journal of Nanomaterials
Volume 2022, Article ID 1988293, 18 pages
https://doi.org/10.1155/2022/1988293

Research Article

The Role of Tetra Hybrid Reinforcements on the Behavior of Aluminum Metal Matrix Composites

Demeke Abay Ashebir,[1] **Getinet Asrat Mengesha**,[1] **and Devendra Kumar Sinha**[2]

[1]*Department of Materials Science and Engineering, Adama Science and Technology University, Adama, Ethiopia*
[2]*Department of Mechanical Engineering, Adama Science and Technology University, Adama, Ethiopia*

Correspondence should be addressed to Demeke Abay Ashebir; demeke.abay@astu.edu.et
and Getinet Asrat Mengesha; getgetuw@gmail.com

Received 12 July 2022; Accepted 18 August 2022; Published 8 September 2022

Academic Editor: Mauro Zarrelli

Hybrid aluminum matrix composites (HAMCs) are a new class of advanced materials that can be customized and engineered to achieve specific properties for specific applications in specific environments. HAMCs find a wide range of popularity in the transportation sector because of lower noise and lower fuel consumption over other materials. This research aims to synthesize, characterize, and test the physicomechanical characteristics of tetra hybrid (SiC, Al_2O_3, Gr, and sugarcane bagasse ash (SCBA)) reinforced HAMCs via powder metallurgy (PM) processing. Tetra hybrid reinforced HAMCs were synthesized using a pure Al matrix with fixed wt% of primary reinforcements (5 wt% SiC and 5 wt% Al_2O_3) and varying wt% of secondary reinforcements such as 0.5, 2.5, 4.5, and 6.5 wt% Gr and 0.5, 2.5, 4.5, and 6.5 wt% SCBA. It mainly focused on phase purity investigation using XRD, thermal analysis using TGA-DTA, and surface area and micropore size analysis using BET and physicomechanical tests to explore the materials' behavior of the newly synthesized HAMCs. The increase in wt% of secondary reinforcements decreases both the density and porosity while increasing the hardness and compressive strength up to a certain level above which it begins to reverse because of the increase in wt% of hard particles of SiC, Al_2O_3, and SCBA. The Vickers hardness and compressive strength of the AS4 HAMC with 10 wt% (SiC+Al_2O_3) and 9 wt% (Gr+SCBA) were improved by 446.40% and 209.75%, respectively. The newly synthesized tetra hybrid reinforced HAMCs showed superior physicomechanical properties compared to pure Al and single and double reinforced HAMCs. As a result, the new tetra hybrid reinforced HAMC material is predicted to have potential applications in automotive, aerospace, defense, and various other structural applications.

1. Introduction

Metal matrix composites are fascinating materials with a wide range of possible uses in the industry [1]. Aluminum metal matrix composites (AMMCs) offer low density, high specific strength and stiffness, better wear resistance, and a regulated expansion coefficient, making them a good fit for the aerospace, automotive, and military industries [2]. In particular, particulate-reinforced aluminum matrix composites (PRAMMCs) are one type of AMMCs, which have low density, lightweight, high specific strength to weight ratio, high stiffness, and excellent wear and corrosion properties. Due to these properties, PRAMMCs have gained attention in the automotive, aerospace, marine, and other industries [3]. PRMMCs also look promising due to their homogenous and isotropic material properties, low cost, and ease to be made using a standard metal process. Such PRAMC materials, which have a variety of uses including lightweight vehicle components, forgings for suspensions, axles, and intricate automobile parts, are exposed to a wide variety of corrosive environments. Light metals such as Mg, Al, Ti, Fe, and Cu and their respective alloys are reinforced with ceramic particulates (such as SiC, Al_2O_3, B_4C, TiC, TiB_2), which shows better physicomechanical, tribological, corrosion, wear, and thermal properties compared to the base materials [4]. In recent years, solid wastes from industrial, agricultural, and postconsumed are used as a secondary reinforcement to these light metals and alloys to enhance

the properties of single reinforced metal matrix composites [5].

The fabrication of hybrid particulate reinforced metal matrix composites (HPRMMCs) is much more complicated than that of single and binary reinforced MMCs. When the type of particulates scales up from single to double and more, many additional difficulties have to be solved and new issues have to be faced. The reaction between ceramic particulates such as SiC and Al_2O_3 or solid waste particulates such as rice husk ash and sugarcane bagasse ash with the metal matrix is still unclear [5]. The inappropriate bonding interface may lead to the failure of the hybrid reinforced metal matrix composites. Clustering of particles is another issue of paramount importance to be solved, especially in large parts [6]. Powder metallurgy (PM) is one of the most important solid-state methods for processing metal matrix composites [7]. In stir casting, the wettability of reinforcing particulates by liquid metal and the density and CTE differences between the matrix alloy and these particulates lead to a nonuniform distribution of the reinforcement phase within the matrix alloy. In addition, the segregation of particles is due to shear effects during solidification and the formation of brittle connections and porosity at the ceramic/matrix interface leads to a deterioration in the mechanical and tribological properties of the composite materials [8]. Furthermore, it has been discovered that the cost and mass of AMCs might well be significantly reduced using hybridized reinforcements without affecting the tribological performance.

Because of the improvements in quality that may be gained, the low cost and availability of particulate materials, and the adaptation of particle-reinforced materials to conventional technology, PRMMCs are now the most widely explored and utilized form of MMC [9]. SiC, Al_2O_3, Si_3N_4, TiC, and B_4C are the most popular particle reinforcing materials [10, 11]. Among the individually reinforced particles in AMCs, SiC and Al_2O_3 exhibit the unique combination properties [12]. In the past few years, HAMCs have received increasing attention for their superior performance. They are regarded as the next generation of composite materials, capable of replacing single reinforced AMCs [13]. Table 1 compares the effects of single, double, and hybrid reinforcements on the distinguishing characteristics of composite materials.

Some of the hard filler particles that are applied to the Al matrix to increase its mechanical strength and wear resistance include silicon carbide (SiC) and alumina (Al_2O_3). However, the usage of single reinforcing particles in an Al matrix might occasionally compromise the physicomechanical property values. Primarily, these reinforcing particles are denser than the Al matrix, increasing the AMCs' density. Second, the ceramic particles are extremely hard, and their abrasive effect increases the tool wear of the mating counterfaces. As a result, such additions diminish the tribosystem's wear resistance while increasing the wear resistance of the AMCs [22]. Thirdly, the inclusion of hard particles raises the hardness of the composites, making AMC machining harder. As a result, it is critical to develop solutions to maintain the favorable effect of ceramic particles while also addressing these issues [23]. Secondary reinforcement is particularly suited for many applications, and its inclusion may make AMC design more versatile and robust. According to a recent HAMC study, the incorporation of Gr particles can reduce composite wear, while agro/industrial waste materials such as sugarcane bagasse ash can be employed to reduce cost and provide lightweight applications [24].

2. Materials and Methods

2.1. Particulate Reinforcement Used to Synthesis HAMCs. The cost of the particulate reinforced composites (SiC, Al_2O_3, and Gr) is less than the fiber-reinforced composites, due to the lower cost of particles [25]. Moreover, the physicomechanical, tribological, and corrosion properties of particulates are generally isotropic. In this research work, four different particulates, namely, SiC, Al_2O_3, Gr, and SCBA (see Figure 1), are used as reinforcement materials. Table 2 provides the raw materials and the rationale for their selection in order to create HAMC materials, which may exhibit superior characteristics to those of the individual components and are anticipated to be a potential candidate material for use in aerospace, automotive, marine, and biomedical applications.

The physicomechanical characteristics of Al, SiC, Al_2O_3, Gr, and SCBA reinforced MMCs are superior to those of the base metal (pure Al) and its alloys [24, 25]. The general physicomechanical properties of Al, SiC, Al_2O_3, Gr, and SCBA are depicted in Table 3.

Hybrid reinforcements outperform double reinforcements, which in turn exhibit greater qualities than single reinforcements. Additionally, the two secondary reinforcements, SCBA and Gr, play a part in lowering the cost and weight while enhancing the necessary qualities. While SCBA is the greatest replacement material for cost and weight reduction as well as enhancing other material qualities including strength, hardness, wear, corrosion, and other features, Gr offers the new HAMC materials a self-lubricating capability.

NA indicates not applicable (or no accessible information).

2.2. Synthesis and Characterization of Sugarcane Bagasse Ash. Sugarcane bagasse ash (SCBA) was collected from the Wonji Shoa sugar factory, which is one of Ethiopia's sugar factories, located in the Oromia region near Adama City at a distance of 25.3 kilometers and 110 kilometers from Addis Ababa. Wonji Sugar Factory, which began production in 1954, was the first and oldest in Ethiopia's sugar sector. As a result, the recently constructed and modernized Wonji Shoa Sugar Factory has a total output of crushing 6250 tons of cane a day, manufacturing 174,946 tons of sugar annually, which will then be increased to 12,500 tons of sugar per year with future development work [36]. Bagasse is defined as the dry pulpy residue left after the extraction of juice from sugarcane. The sugar extracted from sugarcane left behind sugarcane bagasse, when grid powdered to ash, is called sugarcane bagasse ash (SCBA). SCBA is an agro-industrial waste material composed mainly of silicon dioxide. SCBA is one of the most inexpensive and low-density reinforcements available in large quantities as an agro-industrial

Table 1: Comparison of monolithic and single and hybrid reinforced aluminum matrix composites [14–21].

Properties for comparison	Monolithic (pure Al or its alloys)	Material type single reinforced aluminum composite	Hybrid reinforced aluminum composites
Physical	Insufficient	Good	Best
Mechanical	Low-to-medium	Medium-to-high	Very high or superior from the others
Wear	Wearable	Depends on the percentage of reinforcement, still insufficient	Excellent wear resistance
Corrosion	Moderate	Depends on the type of reinforcement, still no enough	Excellent corrosion resistance
CTE	High	Low	Very low CTE

(a) (b)

Figure 1: Raw materials used throughout the research work.

waste by-product during the combustion of waste sugarcane. Equipment used in the preparation of SCBA are crucible, 45 μm size sieve, Becker, sample holder, drying oven, and muffle furnace. The synthesis of SCBA is shown in Figure 2 below.

The largest proportion of the primary components ($SiO_2 + Al_2O_3 + Fe_2O_3$.) in the solid waste SCBA is 86.2% (see Table 4), making it a suitable secondary reinforcement for the creation of innovative MMC materials. Furthermore, XRD measurements of SCBA calcined at 850°C verified the existence of SiO_2 and Al_2O_3, with strong SiO_2 peaks and low Al_2O_3 peaks. Figure 3 depicts the phase identification of SCBA using XRD. As a result, the obtained SCBA fine powder can be used as an effective secondary reinforcing material in the fabrication of novel tetra hybrid reinforced HAMC materials.

2.2.1. Synthesis of HAMCs Using the PM Process

(1) Chemical Composition and Sample Designation in the Synthesis of HAMCs. In this study, fine Al powder with particle size 45 μm and reinforcement fine powders with particle size 45 μm, namely, SiC, Al_2O_3, Gr, and SCBA, are employed. Following the selection of matrix and reinforcement materials, the next critical duty is to blend or mix them with the optimal composition. The powder metallurgy technique was used for the synthesis of HAMCs from the Al matrix and using SiC and Al_2O_3 as primary reinforcements, and Gr and SCBA as secondary reinforcements. Using SiC and Al_2O_3 as primary reinforcements within the range of 3–10 wt% yields superior physical, mechanical, and tribological properties [20, 37].

The composition and sample design are shown in Table 5, and the PM process parameters used throughout the investigation are shown in Table 6.

Because of the hydraulic pressing machine's capacity, the dimensions of the specimens produced are limited to cylindrical specimens with short lengths. The dimensions of all specimens are shown in Figure 4.

(2) Steps in the PM Process. The PM technique is one of the most cost-effective methods for creating near-net particle

Table 2: Raw materials and reasons selected for HAMC production.

No.	Raw materials		Reasons for the selection to use in HAMCs	Ref.
1.	Matrix	Pure Al	(i) Lightweight, and low density, but the low melting point hinders its use in the high-temperature application. (ii) High ductility, malleability, and toughness with low strength, soft, and low wear and friction resistance	[26]
2.	Reinforcements	SiC	(i) High hardness and mechanical stability at high temperatures because of its very high melting point (ii) Excellent thermal conductivity and low coefficient of thermal expansion, (iii) Excellent resistance to chemical, wear, thermal shock, corrosion, and oxidation	[26]
3.		Al_2O_3	(i) High hardness and mechanical stability at high temperatures because of its very high melting point (ii) Excellent thermal conductivity and low coefficient of thermal expansion (iii) Excellent resistance to chemical, wear, thermal shock, corrosion, and oxidation	[26]
4.		Gr	(i) Lightweight, low density (ii) Superior solid-lubricating material (iii) High friction resistance (iv) Low cost	[26–28]
5.		SCBA	(i) Lightweight, low density (ii) Easily available as it is a solid waste material (iii) A promising alternative for MMCs	[29, 30]

Table 3: Physicomechanical properties of the raw materials [26, 31–35].

Materials	Al (pure)	SiC	Al_2O_3	Gr	SCBA
Appearance (form)	White powder	Dark gray powder	White powder	Black powder	Black-gray
Density (g/cm^3)	2.7	3.2	3.96	1.8	0.8–1.477
M.W.	26.98	40.096	101.96	12.01	NA
Melting pt. (°C)	660	2730	2054	3652–3697	1350
Particle size (μm)	45	45	45	45	45
Vickers hardness (MPa)	167	20000–27000	11000–17000	67	NA
Compressive strength (MPa)	110	2800	2500	20–200	NA
Tensile strength (MPa)	130-195	310	221	3–33	NA
Young's modulus (GPa)	70	410	379	380–470	NA
Purity (%)	99.5	97	97	98	NA

einforced MMCs, providing for increased flexibility, lower production costs due to reduced machining time, and lower scrap losses [39, 40]. As Mazen and Ahmed [41] and Dubey et al. [42] discovered, the PM production approach provides higher consistency in the distribution of the reinforcing material, which reduces clustering and improves mechanical characteristics. The following are the steps in the powder metallurgy technique [43]. Powder mixing, powder compaction, and sintering process are the three essential phases in powder PM operation.

(1) Blending (or Mixing): The HAMCs were mixed using a high-energy planetary blending machine with 10 wt% of primary reinforcement (i.e., 5 wt% SiC and 5 wt% Al_2O_3) and different wt% of secondary reinforcement (0.5, 2.5, 4.5, and 6.5 wt% for each of Gr and SCBA) [44]

(2) Compaction. To produce a cylindrical form of the solid green body at room temperature, the blended HAMCs were compressed in a uniaxial hydraulically operated machine. A compaction pressure of 60 MPa was used to compact the test materials. As shown in Figure 5, a self-prepared die and punch assembly with a maximum die diameter of 20 mm was employed during bulk HAMC fabrication

(3) Sintering. TGA-DTA investigation of milled HAMC powders revealed that the HAMCs undergo phase change at temperatures over 661.89°C. As a result, the sintering temperature should be less than

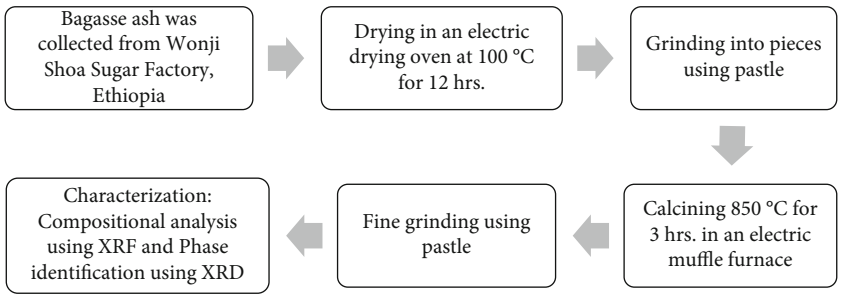

Figure 2: Synthesis of SCBA fine powder particulates.

Table 4: XRF analysis of SCBA.

Composition	SiO_2	Al_2O_3	Fe_2O_3	CaO	MgO	Na_2O	K_2O	MnO	P_2O_5	TiO_2	H_2O	LOI
SCBA (%)	65.50	16.52	4.08	0.01	0.01	0.01	1.5	0.1	0.5	0.24	0.66	10.87

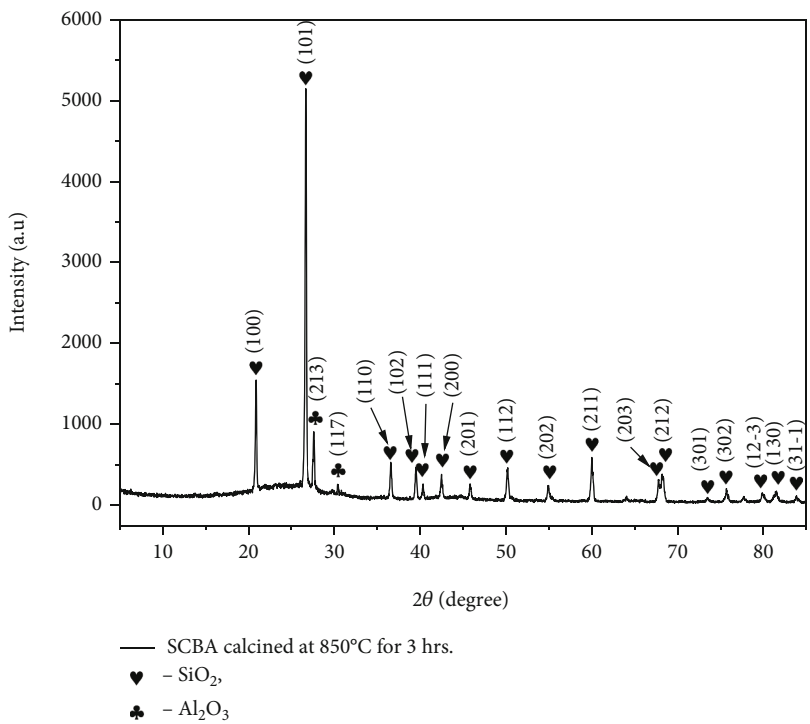

Figure 3: XRD graph of SCBA calcined at 850°C for 3 hrs.

Table 5: Chemical composition and sample designation used in the HAMCs.

Sample designation	Al (wt%)	SiC (wt%)	Al_2O_3 (wt%)	Gr (wt%)	BA (wt%)
Pure Al	100	0	0	0	0
AS1	90	5	5	0	0
AS2	89	5	5	0.5	0.5
AS3	85	5	5	2.5	2.5
AS4	81	5	5	4.5	4.5
AS5	77	5	5	6.5	6.5

661.89°C. The samples were heated from room temperature to 550°C at a rate of 10°C/min for 55 mins, then maintained at that temperature for 3 hrs

To reduce oxidation during heating, the samples were sealed with Al foil. The samples were then allowed to cool to room temperature within the furnace before being exposed to the environment. Figure 6 depicts the full experimental setup of the HAMCs synthesis.

3. Results and Discussions

3.1. Characterization of HAMCs

Table 6: Powder metallurgical process parameters for this study [38].

Samples	Chemical composition	PM processing parameters
Pure Al	Al	(1) Milling time = 2 hrs. (2) Compacting pressure = 60 MPa (3) Sintering temperature = 550°C (4) Sintering time = 3 hrs.
AS1	$Al/5SiC/5Al_2O_3$	
AS2	$Al/5SiC/5Al_2O_3/0.5Gr/0.5SCBA$	
AS3	$Al/5SiC/5Al_2O_3/2.5Gr/2.5SCBA$	
AS4	$Al/5SiC/5Al_2O_3/4.5Gr/4.5SCBA$	
AS5	$Al/5SiC/5Al_2O_3/6.5Gr/6.5SCBA$	

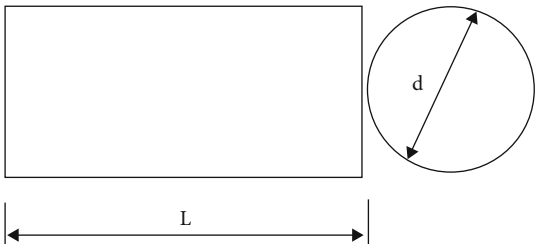

Figure 4: All specimens' dimensions.

3.1.1. Phase Analysis of the HAMCs. The XRD patterns of the HAMC specimens were analyzed using Origin and HighScore Plus software [46]. Figure 7(a) depicts the XRD graph of the HAMC powders following milling before compaction and sintering were performed. The graph shows that there is a dominancy of the matrix and other reinforcements' significant peaks are not shown, which ascribes that in the milling process, there was no undesirable interfacial chemical reaction between the hybrid reinforcements and the matrix [47]. As shown in Figure 7, Al with a cubic crystal structure with $a = b = c = 4.0500\mathring{A}$ and $\propto = \beta = \gamma = 90^\circ$ with an experimental density of 2.675 g/cm^3 can be detected in the HAMC samples, regardless of whether it is before or after sintering. However, in the composite shown in Figure 7(b), the peaks corresponding to distinct phases are recognized as Al, SiC, Gr, Al_2O_3, SiO_2, and Fe_2O_3. The presence of SiO_2, Al_2O_3, and Fe_2O_3 in the HAMCs is highly correlated with the presence of SiO_2, Al_2O_3, and Fe_2O_3 in the SCBA [48, 49]; this is strongly associated with XRF results depicted in Table 4.

The minor peak of Fe_2O_3 (JCPDS card number: 00-046-1212) was shown for AS2 and AS3 at $2\theta = 18.062^\circ$ corresponding to the (111) crystallographic plane, but in other samples, this oxide is not further shown as it is dominated by the other oxides such as Al_2O_3 and SiO_2, which comes from SCBA [50]. The minor peak of Gr is shown at angles $2\theta = 26.603^\circ$ which corresponds to (111) (JCPDS card number: 00-025-0284), and 21.895° which corresponds to the (101) crystallographic plane of SiO_2 (JCPDS card number: 00-029-0085). The minor peaks at angles $2\theta = 36.651^\circ$, 60.034°, and 71.772° correspond to the (006), (103), and (116) crystallographic planes, indicating the presence of SiC (JCPDS card number: 01-073-0603). The minor peaks Al_2O_3 were also shown at angles of 35.324°, 45.790°, and 66.763° (see AS3, AS4, and AS5) corresponding to (104), (111), and (211) crystallographic planes. The presence of Al_2O_3 and SiO_2 ascribes to the presence of SCBA, which confirms that SCBA could be a promising material for the development of novel tetra hybrid reinforced HAMC materials with Al as a matrix for the application of aerospace and automotive components [47, 49, 51].

3.1.2. TGA-DTA Thermal Behavior of HAMCs. The weight change of HAMC materials as a function of temperature was investigated using thermogravimetric analysis (TGA), whereas the phase changes of the HAMC material as a function of temperature were investigated using differential thermal analysis (DTA) [52]. Dehydration, decomposition, oxidation, and other processes cause phase transition in composite materials [53, 54].

Figure 8(a) depicts the TGA-DTA curves for the AS1 HAMC sample. At 25°C, the TGA curve represents 100 wt% weight. The weight of the material does not change as the heating temperature increases, albeit there was a 0.01–0.02% increase in mass from 80 to 220°C, which might be related to the impurities contributed by the inert nitrogen atmosphere. Heating from 220 to 560°C starts with a minor loss in mass due to the decomposition of material on the temperature rise, but from 600 to 1000°C, the pattern reveals a gradual increase in weight, with a total of 1.00% weight gain at 1000°C. As can be observed from Figure 8(a), the weights of all powders rapidly increased with increasing temperature, from approximately 860.10 to 1000°C. The formation of oxides, which were generated due to the exothermic reactions between Al and oxygen, was assumed to have caused the increase in weight [55]. In addition, due to the heat involved in the TGA process, Al and oxygen reacted to form Al_2O_3, and their presence in the composites was confirmed using the XRD patterns. A wide variety of alumina ceramics has been studied for reactions and wettability with different metals [56]. It is generally recognized that alumina cannot be wetted by pure Al below about 800°C. However, as wetting transitions are very sensitive to the nature of the substrate, quality of the atmosphere, and other factors, the temperature for wetting transitions is seldom universal and well defined. The stationary contact angle of Al on single-crystal alumina decreases linearly in the 800–1000°C temperature range, a typical wetting behavior in a nonreactive metal/alumina system [56]. Therefore, the formation of Al_2O_3 will not hurt the behavior of HAMC.

As shown in Figure 8(a), the DTA plot indicated one endothermic peak of 664.10°C, indicating the site of phase

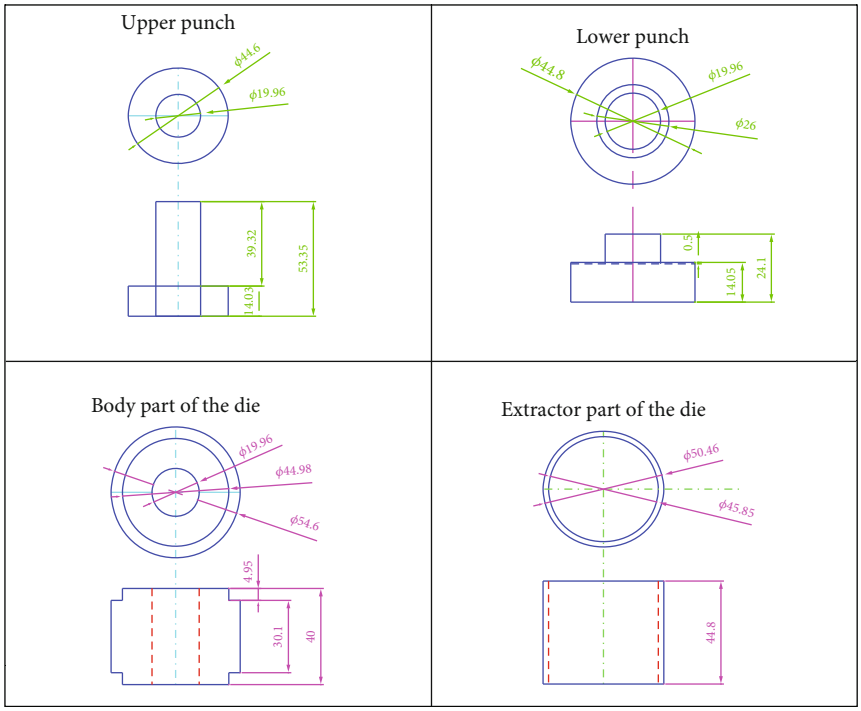

Figure 5: Die and punch assembly.

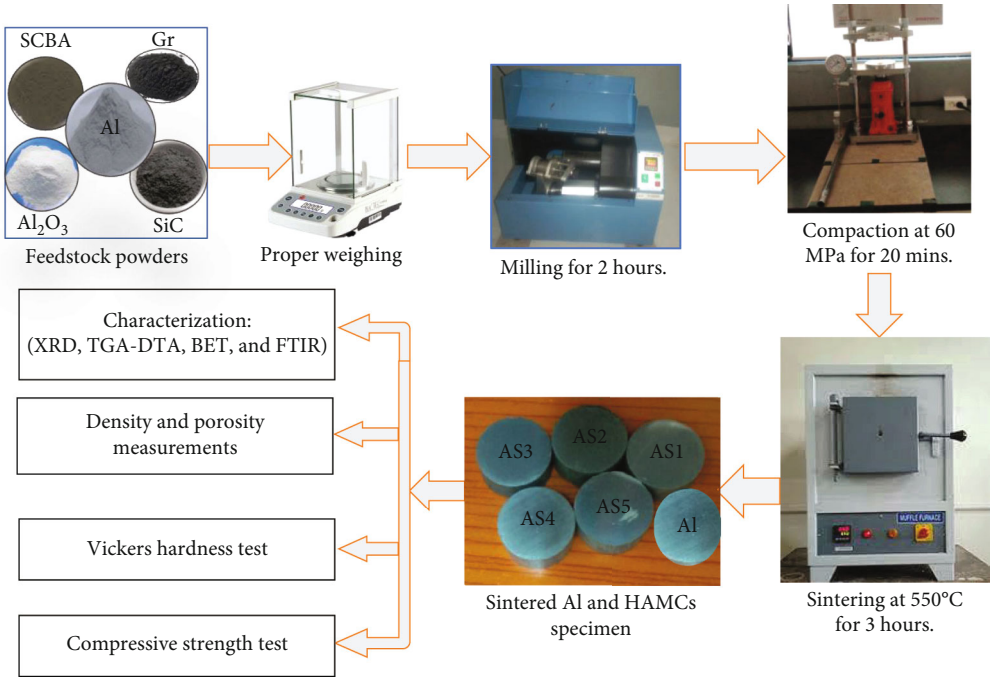

Figure 6: Experimental setup for the synthesis of HAMCs using powder metallurgy process [45].

change. The thermal conduction and temperature of diffusivity of SiC and Al_2O_3 particles are lower than those of Al, allowing them to store rather than convey heat. As a result, the temperature of these reinforcing particles in Al (SiC + Al_2O_3) HAMCs is always somewhat higher than that of Al. The HAMCs' total softening/melting was delayed by the SiC and Al_2O_3 particles. The more SiC and Al_2O_3 particles are added, the greater the softening/melting resistance. Because of this, there is more thermal stability in these HAMCs compared to a more reactive base material. The

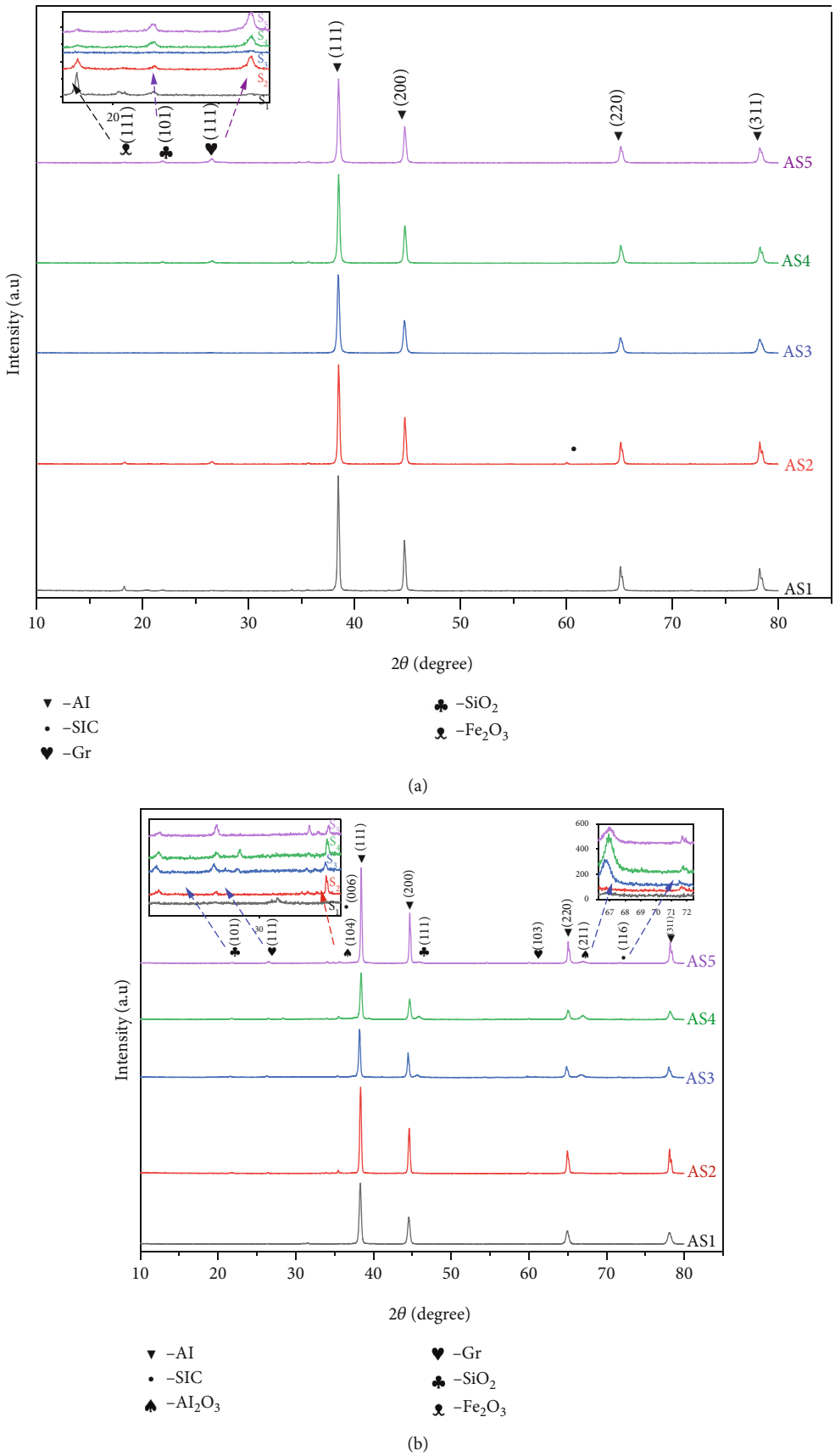

Figure 7: XRD results of HAMCs of (a) before sintering and (b) after sintering.

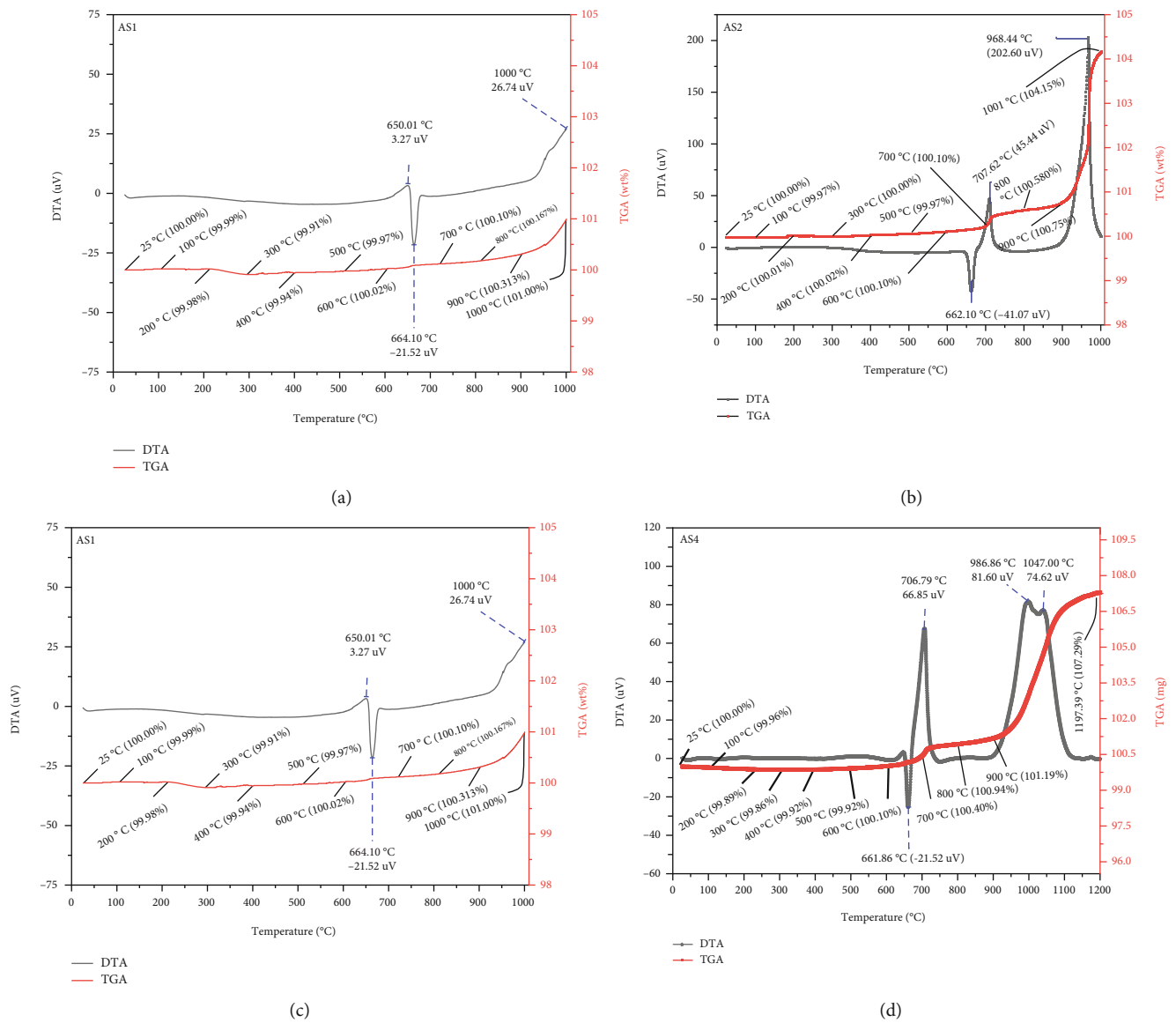

Figure 8: Continued.

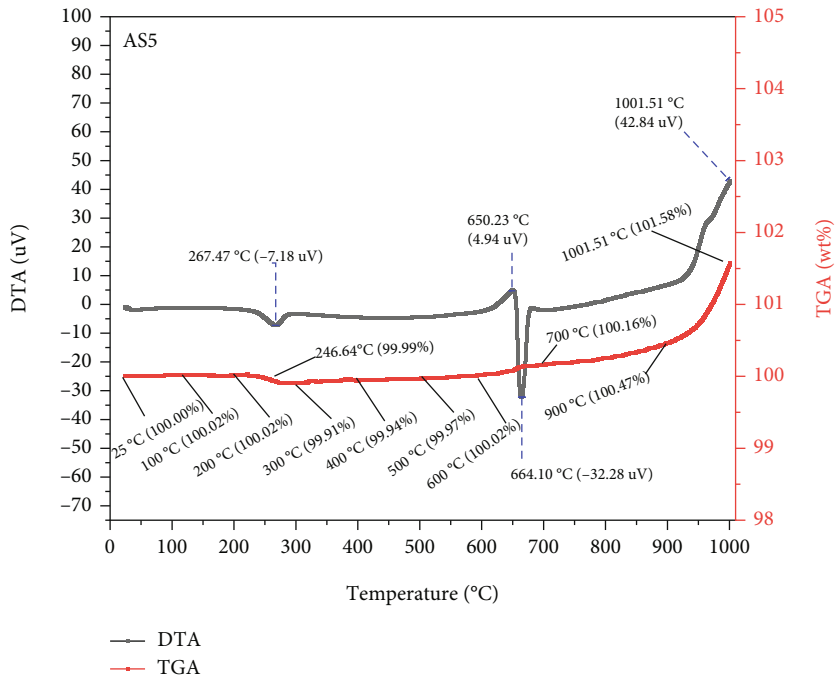

(e)

Figure 8: TGA and DTA graph of (a) AS1, (b) AS2, (c) AS3, (d) AS4, and (e) AS5 of HAMC samples.

DTA curve also shows an exothermic peak at 650.01°C. This could signify that there was some weight gain at this instant of temperature [52].

Figures 8(b)–8(e) represent the TGA-DTA plots for AS2, AS3, AS4, and AS5 with the addition of secondary reinforcements (Gr and SCBA) into AS1 HAMC. The plots shown in Figure 8(b) evaluate the TGA and DTA of the AS2 HAMC sample. These plots were employed to see the effect of secondary reinforcement on the thermal stability and phase change of the AS1 HAMC. There is no more change in the weight gain ranges, although some slight variations have happened in TGA curves. As can be observed in Figure 8(b), in the first stage, the material loses moisture and impurities. From 285 to 485°C, the thermal stability is more than that of AS1, which is one of the positive impacts of secondary reinforcement on the HAMCs. The endothermic peaks were shown at 662.10°C which shows the phase transformation temperature; due to the hygroscopic nature of the secondary reinforcement materials (SCBA), the mass of the composite gradually drops with a total mass loss of 0.03% as the temperature rises, stabilizing between 540.56 and 590.69°C before increasing mass from 601.16 to 1000°C [52].

As shown in Figure 8(b), the DTA plot indicated one endothermic peak of 662.10°C, indicating the site of phase change. Due to the addition of secondary reinforcements, there is an exothermic peak at 707.62°C. This exothermic peak in AS2 is a higher temperature than AS1 HAMC (see Figures 8(a) and 8(b)). Furthermore, the weight gain in AS2 is more than in AS1; it is because of the SCBA, which has more oxides that can form Al_2O_3 with pure Al [57]. After 985°C, the HAMC starts thermal stability, which shows that AS2 is more thermal performance than Al [57]. As can be observed in Figure 8(c), the endothermic and exothermic peaks of AS3 are increased relative to AS2. Between 60 and 700°C, there is little fluctuation in weight due to the elimination of impurities and moisture at the beginning and oxidation at the end. When the temperature rises from 700 to 1000°C, there is a noticeable increase in weight gain. There was no notable weight loss or gain throughout this test, indicating that the material is thermally stable. Furthermore, the little change among temperatures up to 630°C demonstrates heat flow stability.

At low temperatures up to 100°C, weight loss may be caused by moisture escaping, which turns to vapor when heated, and at high temperatures, some of the impurities present in the second reinforcing material (SCBA) may burn off, resulting in mass loss [54]. It demonstrates that the weight gain is started at around 600°C and continues up to 1200°C. The warm strength of hybrid reinforcement is higher than that of Al. Hence, as the wt% of these hybrid reinforcements in the HAMCs expands its introduction of start temperature increments or gets fortified, Al may respond to barometrical oxygen to frame an Al_2O_3 film which is stable, definitely following, and dense. The DTA plot in Figure 8(d) at 661.89°C shows the transformation phase, i.e., the point where Al in HAMC materials will be transformed from the solid state to the molten state [53]. Weight progressively rises before plateauing as the metallic component begins to oxidize. Because there is no more accessible material in contact with oxygen, the plateau develops.

Table 7: Summary of the thermal behavior of the HAMCs.

Samples	Total weight gain (%)	TGA (thermal stability range in °C)	DTA (phase transformation) (°C)
AS1	1.00	300–620	664.10
AS2	4.15	300–620	662.10
AS3	1.84	300–620	661.89
AS4	7.29	300–620	661.89
AS5	1.58	300–620	664.10

The TGA-DTA plots in Figure 8(e) (AS5) are almost the same as in Figures 8(b) and 8(c) up to 600°C. The DTA curve in Figure 8(e) includes two endothermic peaks at 267.11°C and 664.10°C, indicating that the phase change occurs at these temperatures. The first endothermic peak could be because of the phase change of some volatile impurities on the surface of the sample and the inert gas environment. The phase change on the second peak could be because of the melting temperature of the base metal (pure Al). Because of the influence of increased SCBA levels, which may have larger impurity contents, the first endothermic peak in AS5 is not seen in any other HAMC samples. The secondary reinforcement percentage of AS5 is higher (6.5 wt% Gr and 6.5 wt% SCBA).

The following major points summarize the TGA-DTA analysis results. The TGA-DTA curves for HAMCs are shown in Figures 8(a)–8(e). The thermal behavior of HAMCs during heating was depicted by these curves. The loss of moisture causes the initial drop in the mass of every sample up to 100°C. While the little loss in mass is due to material disintegration as the temperature rises, an increase in mass may be detected elsewhere, which is due to composite oxidation. The peak of the DTA in the curves depicts the phase transition during the heating or cooling cycle. Because the tetra hybrid reinforced HAMCs have lower thermal conductivity and temperature of diffusivity than Al, they can store heat rather than transport it [57]. As a result, the temperature of these reinforcing particles in HAMCs is always somewhat higher than that of Al. The HAMCs' total softening/melting was delayed by the SiC, Al_2O_3, and SCBA particles. The more SiC, Al_2O_3, and SCBA particles are added, the greater the softening/melting resistance.

The DTA displays endothermic peaks ranging from 661.89 to 664.10°C, indicating phase changes from the liquid state (melting). Because both phases (matrix and reinforcement) have their own identity in the material and exist in a free state, the melting point does not alter much. During heating, the matrix material softens and ultimately melts, leaving the tetra hybrid reinforcements (SiC, Al_2O_3, Gr, and SCBA) in the melt. Due to the existence of tetra hybrid reinforcement, a minor difference in the heat of fusion may be noticed (SiC, Al_2O_3, Gr, and SCBA). Composites do not melt at a fixed temperature, but rather at a variety of temperatures. Due to the addition of tetra hybrid reinforcements (SiC, Al_2O_3, Gr, and SCBA), significant modifications in the melting temperature can be noticed, as indicated in Table 7. Table 7 shows the characteristics of the thermal behavior of the produced HAMCs, including weight loss/gain, the range of material thermal stability determined by TGA, and phase transition by DTA.

The oxidation of AS4 is higher than that of all others, and at a higher temperature, it shows more thermal stability, while AS1 has lower weight loss as the primary reinforcements are more chemical and thermal stable than secondary reinforcements.

The range of thermal stability increases with the addition of hybrid reinforcement particulates; for example, 10% of primary reinforcement and 1% of secondary reinforcement reinforced HAMCs were stable at the temperature range of 300–620°C above the range of material stability for the base metal (pure Al). When compared to base metals (Al with a melting temperature of 660°C), all HAMCs exhibit superior thermal resistance and material stability at higher temperatures ranging from 300.560 to 610.00°C. According to Table 7, the phase transition temperature is between 660 and 670°C. Based on this information, the new tetra hybrid reinforced HAMCs' sintering temperature must be less than 0.7–0.9% of the phase transformation temperature (melting point) of the given material. These TGA and DTA analyses were well supported by previous research [58, 59]. Based on the results, the sintering temperatures of the novel tetra hybrid reinforced HAMCs were determined to be 400, 450, 500, and 550°C, which are all within the specified domain.

3.1.3. FTIR Characterization of HAMCs. The chemical properties of HAMCs were investigated through FTIR analysis, and the peak values were identified. The FTIR was recorded at a spectrum resolution of 4000–400 cm^{-1} using a Bruker Vertex 70 photometer. For identifying different chemical functional groups present in a HAMC sample, FTIR is a standard method as a nondestructive testing tool [60]. The absorption of radiation and the measurement of the vibrational changes of molecules and multiatom ions are the foundations of infrared spectroscopy [61]. This approach may be used to determine the chemical bonding on the surface of HAMCs.

In the region of 1000–500 cm^{-1}, the vibration of the main functional groups of Si-O and Al-O was observed. The peak observed around 550 cm^{-1} is characteristic of Fe-O vibrations. The HAMCs exhibit peaks at 510 and 1082 cm^{-1} that correspond to the Al-O bonds. The band at around 1100–1010 cm^{-1} is assigned to Si-O stretching vibrations, and the absorption bands at 914, 540, and 470 cm^{-1} are attributed to Si-O-Si bending vibrations. These bands are assigned to the symmetric and asymmetric vibrations of valence bonds Si-O-Si [62, 63]. The doublet at 780–798 cm^{-1} is due to Si-O-Si intertetrahedral bridging bonds in SiO_2 [63, 64]. The drop in IR transmittance in the wavenumber interval between 400 and 900 cm^{-1} is due to the absorption produced from Al-O stretching. The weak IR band around 1177 cm^{-1} is from the Si-O-Si stretching of silica species. The peaks at 1702, 1594, and 1408 cm^{-1} are due to the presence of the sp^2 bond of graphite [60]. The FTIR spectrum peaks 883, 2353, and 2374 correspond to the Si-C group [61]. As seen in the FTIR spectra

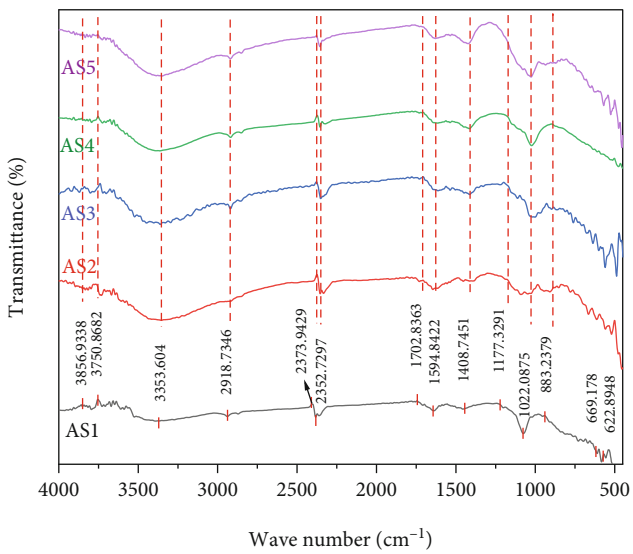

Figure 9: FTIR spectra of the HAMC samples.

Table 8: BET results of AS1 and AS4 HAMC powder samples.

Sample	Surface area (m^2/g)	Pore volume (cm^3/g)	Pore size (nm)
AS1	581.542	0.03815	0.1684
AS4	290.866	0.01316	0.1324

of all HAMCs in Figure 9, a broad absorption peak at 3353 cm^{-1} corresponds to the stretching vibration absorption peak of Al-OH [65]. Large bands around 3400, 3700, and 3856 cm^{-1} are also observed, due to the -OH groups adsorbed on the HAMC surface [65].

3.1.4. Brunauer-Emmett-Teller (BET). As seen in Table 8, the AS1 HAMCs have a greater surface area, pore volume, and pore size than the AS4 HAMCs. The AS1 HAMC sample's large specific surface area might be attributable to the inclusion of hard particles such as SiC and Al_2O_3 in the AS1 HAMC sample. The HAMC materials also contain the Dubinin-Radushkevich (DR) method micropore with sizes and volumes of 0.1684 nm and 0.03815 cm^3/g for AS1 and 0.1324 nm and 0.01316 cm^3/g for AS4, according to the data in Table 8. The AS4 HAMC sample has a smaller surface area and micropores due to the inclusion of 4.5 wt% Gr and 4.5 wt% SCBA secondary reinforcements. This is due to an increase in particulate uniform distribution within the matrix. Moreover, Gr aids in the rearrangement and movement of hard particles inside the base materials, resulting in increased hardness and decreased porosity [25].

3.1.5. Physicomechanical Behavior of HAMCs

(1) Density and Porosity Measurement. The main physical testing conducted on Al and HAMCs comprises density and porosity studies. The acquired samples are typically weighed in the air and distilled water of known density. Porosity is a measure of the amount of vacant space between particulates within the sample, and it is the ratio of the volume of space to the total volume of the composite material, whereas density is the ratio of mass to the overall volume of a composite material. The Archimedes principle is widely used to calculate density [66]. At room temperature, the density and porosity of Al and HAMCs were investigated to determine the extent of void growth in the matrix, as well as the widening of the preceding voids, to achieve excellent physical and mechanical characteristics in the HAMCs. A distilled water immersion technique is used to determine density. The densities calculated from the observed weights were then compared to the theoretical rule of mixture (ROM) density to estimate the percentage of porosity. Due to the increased density of the hard SiC and Al_2O_3 particles, the incorporation of primary reinforcement into pure increases both the density and porosity of HAMCs. Figure 10 demonstrates how the experimental density, theoretical density, and % void content of the HAMC specimen vary with different compositions. The AS1 HAMC sample has greater theoretical and experimental density than the base metal due to the inclusion of SiC and Al_2O_3, which are harder and stronger particles than Al. With the addition of secondary reinforcement, both 0.5 wt% Gr and 0.5 wt% SCBA particulates in AS1 start decreasing in density and porosity of HAMC samples, due to the lower density of Gr (2.28 g/cm^3) and SCBA (1.48 g/cm^3) compared to the primary reinforcements, SiC (3.20 g/cm^3), Al_2O_3 (3.96 g/cm^3), and base matrix, Al (2.70 g/cm^3). As can be seen in Figure 10 below, tetra hybrid reinforced HAMCs show lower density than AS1 HAMC and Al samples and goes on decreasing as the composition of Gr, and SCBA increases up to AS4. The AS4 HAMC sample had the lowest % void content, with 4.5 wt% Gr and 4.5 wt% SCBA. Gr is a solid lubricant that enables filler particles in the Al matrix to move and reorganize [67]. As a result, raising Gr contents in HAMCs to a certain limit is considered beneficial for obtaining minimal porosity [68]. According to Figure 10, both the experimental and theoretical densities of the HAMC are following each other, indicating the applicability of the PM process, and this is closely associated with prior studies [69]. Because of the lower density of SCBA and Gr secondary reinforcements, the density of the HAMC samples from AS1 to AS5 decreases as the SCBA and Gr particulate content increases. However, the porosity exhibits a slight perturbation, with AS4 having the lowest porosity of all samples; this result is significantly associated with XRD data. More reinforcement phases are visible in the XRD data of the AS4 HAMC sample, indicating that the tetra hybrid reinforcements are more uniformly distributed inside the matrix. This is also seen in the developed HAMC material's enhanced hardness, strength, corrosion, and wear resistance, as well as in previous findings [19]. The increased wt% of secondary reinforcement caused increased porosity due to the increase in SCBA content, which could initiate cracking in the HAMCs, and the Gr content above the optimal range could also cause more porosity because of its lightweight and inability to easily rearrange and move with the Al, instead of accumulating in some portions, causing the partial

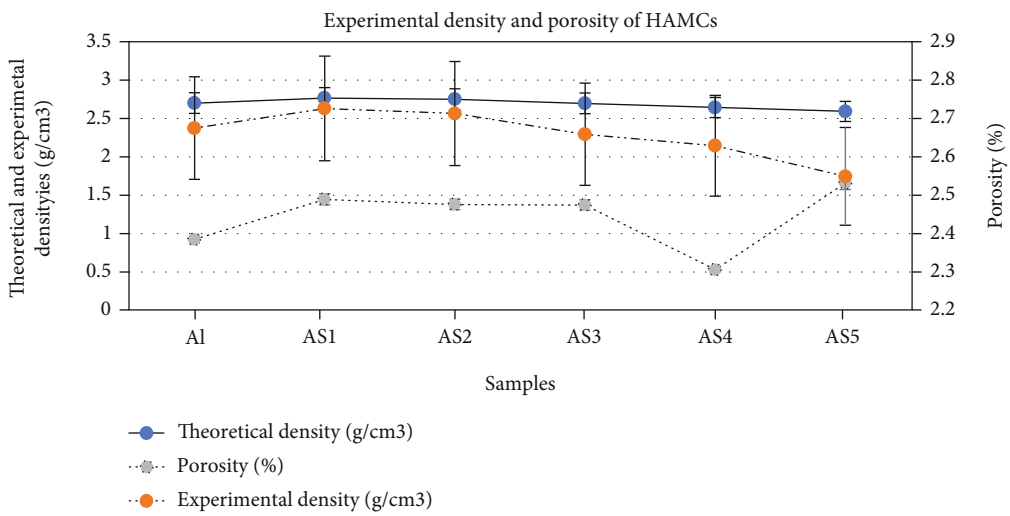

Figure 10: HAMC experimental density variation with reinforcement type and wt%.

distribution of hybrid reinforcements in the Al matrix. Table 9 shows the theoretical and experimental densities and porosity of Al and HAMC samples.

In HAMCs, a higher void content is unfavorable and indicates low quality. When using a HAMC material with a high void content, it has an impact on its properties and performance. As a result, the density of HAMCs might be considered a fundamental measure for assessing their quality.

(2) Vickers Microhardness (HV). The five trials and average Vickers microhardness values of the six sintered HAMCs samples are shown in Table 10, and the average HV values are shown in Figure 11. The addition of 10 wt% (5 wt%SiC + 5 wt%Al_2O_3) hard particle base metal (Al) enhances the hardness by 2.34 times, with 134.49% of improvement, as indicated in Figure 11. Because of the hard SCBA fine particulates, there is an increasing trend in hardness from AS1 to AS4 with the addition of secondary reinforcements up to 9.0 wt% (4.5 wt% of Gr, and 4.5 wt% of SCBA) of fine particulates, confirming that SCBA is a promising material capable of substituting hard particles (ceramic particulates) to be used as reinforcement. This is a large advance since agro-industrial solid wastes such as SCBA are light in weight, low in density, and widely available, while still ensuring a safe and clean environment. The greatest hardness value observed in the AS4 HAMC sample is 358.66, which is 5.464 times greater than the average hardness value of the base metal, or it is 446.40% enhanced with an increase to 9 wt% (4.5 wt%Gr + 4.5 wt%SCBA), after which the hardness trend begins to decline. The inclusion of softer reinforcing (Gr) particles might cause a reduction in hardness. This finding is well associated with earlier research [48, 70]. The size, volume, and type of reinforcement particulates are the most important factors influencing hardness [71]. The average HV improvement is depicted in Figure 11(b). Table 10 displays the average HV values of five trials of HAMCs with fixed amounts (5 wt%) of SiC and Al_2O_3 and changing wt% of SCBA and Gr fine particles.

The greater microhardness of the SiC, Al_2O_3, and SCBA (that comprises SiO_2, Al_2O_3, Fe_2O_3, and TiO_2) can be ascribed to the improvement in the hardness of the HAMCs with increasing reinforcing content. This is strongly correlated with previous research [72, 73]. Because of the inclusion of higher modulus powders, smaller grain sizes, and numerous reinforcements, the hardness of the hybrid composites was greater than that of the single and double reinforced composites, which was higher than that of the base metal. Moreover, the high cost and limited supply of conventional ceramic reinforcing materials, especially in developing countries, have remained a major problem associated with the development of HAMCs. Using two or more reinforcing materials gives room for the possible reduction of cost coupled with property optimization in HAMCs [22].

(3) Compressive Strength Testing. According to Table 11 and Figures 11(a) and 11(b), incorporating tetra hybrid reinforcements into the base metal during HAMC manufacture boosted their compressive strength. This might be because the microstructure acts as a barrier to grain dislocation [74]. The use of hybrid reinforcement was shown to boost the compression strength. When additional Gr and SCBA particles were introduced, the inter-particulate space between them shrank, causing the dislocation pack to rise. Moreover, compression improved from 134.49% (for AS1) to 209.75% (for AS4).

Matrix strengthening caused by a reduction in composite grain size and the creation of a considerable density in the matrix due to variations in thermal expansion coefficients between matrix and hybrid reinforcements can be attributed to HAMCs. The compressive strength of the HAMCs slightly increased while the density is decreasing; this might

Table 9: Density and porosity results of the developed HAMCs.

Sample	Chemical composition	Theo. density (g/cm^3)	Exp. density (g/cm^3)	Porosity (%)
Al	Pure Al metal	2.700	2.675	0.926
AS1	Al/5SiC/5Al_2O_3	2.766	2.726	1.446
AS2	Al/5SiC/5Al_2O_3/0.5Gr/0.5SCBA	2.751	2.713	1.381
AS3	Al/5SiC/5Al_2O_3/2.5Gr/2.5SCBA	2.696	2.659	1.372
AS4	Al/5SiC/5Al_2O_3/4.5Gr/4.5SCBA	2.643	2.629	0.530
AS5	Al/5SiC/5Al_2O_3/6.5Gr/6.5SCBA	2.592	2.549	1.659

Table 10: Five trials and average microhardness values of the sintered HAMC sample.

Sample	Chemical composition	HV_1	HV_2	HV_3	HV_4	HV_5	$HV_{Average}$
Al	Pure Al metal	63.90	66.10	66.00	65.70	66.50	65.64
AS_1	Al/5SiC/5Al_2O_3	153.00	159.40	153.20	150.00	154.00	153.92
AS_2	Al/5SiC/5Al_2O_3/0.5Gr/0.5SCBA	201.10	199.00	193.80	200.10	194.80	197.76
AS_3	Al/5SiC/5Al_2O_3/2.5Gr/2.5SCBA	197.90	204.40	199.00	204.40	206.60	202.46
AS_4	Al/5SiC/5Al_2O_3/4.5Gr/4.5SCBA	380.60	402.60	332.60	348.00	329.50	358.66
AS_5	Al/5SiC/5Al_2O_3/6.5Gr/6.5SCBA	167.40	177.60	192.30	170.20	176.30	176.76

be one of the positive effects of hybrid reinforcements [44]. The compressive strength tests follow the same pattern as the Vickers hardness results; such results are unique in tetra hybrid reinforced HAMCs due to the customizability behavior of hybrid reinforcements used in the fabrication of HAMCs. Moreover, the testing findings revealed that AS4 with 10% primary reinforcement (SiC and Al_2O_3) and 9% secondary reinforcement (Gr and SCBA) of HAMCs had the highest potential in terms of decreased porosity and better compressive strength. It can be stated that 10% of the primary reinforcements (SiC and Al_2O_3) and 9% of the secondary reinforcements (Gr and SCBA) of HAMCs had superior physicomechanical characteristics when compared to other compositions. Particulate reinforced AMCs outperform conventional materials in terms of hardness, tensile and compressive strength, and tribological properties [75]. Furthermore, due to the composite's single reinforcement, the characteristics of AMCs cannot be adjusted. However, HAMCs may be customized to meet specific needs by selecting appropriate reinforcements. Because of its ease of use and the ideal combination of configurable tribological and mechanical properties, high strength-to-weight ratio, and environmental friendliness, HAMCs have become a popular choice for the aerospace, automotive, sporting, and electronics industries [75].

The percentage of improvement in material properties was calculated using the following equation;

$$\text{Improvement}(\%) = \frac{\text{New}(X_i) - \text{Original}(X_i)}{\text{Original}(X_i)} \times 100, \quad (1)$$

where the original (X_i) is the average value of base metal Al and X_i is the test (HV, CS).

The new (X_i) is the average value of the HAMC samples. All improvement percentages in this research are based on this equation. Based on this, the improvement (%) of HV and CS for each HAMC sample is the plot shown in Figure 11(b). Potential applications for the manufactured HAMC material include aerospace components, military, and various automotive-related industries.

4. Conclusion and Future Perspectives

In the present study, a powder metallurgically synthesized tetra hybrid reinforced HAMC has been studied. The main findings of this study can be summarized as follows:

(i) The major peaks in the XRD findings are Al, while the hybrid reinforcements appear as minor peaks, indicating that HAMCs were effectively synthesized by the PM technique. The TGA-DTA results revealed that HAMCs have more thermal stability and a wider range of phase change temperatures than the base material (Al)

(ii) The BET results revealed that the AS4 HAMC had a smaller surface area and micropores than the AS1 HAMC. Decreased micropore size resulted in a lower surface area

(iii) The density and porosity of the tetra hybrid reinforced HAMCs decreased slightly as the wt% of secondary reinforcement increased, but the hardness and compression strength of the HAMCs increased up to 9 wt% of secondary reinforcement (Gr and SCBA) and then reversed with further increases above 9 wt%. The Vickers hardness and compressive strength of AS4 were enhanced by 5.464 and 3.100 times, respectively, over the basis material (Al)

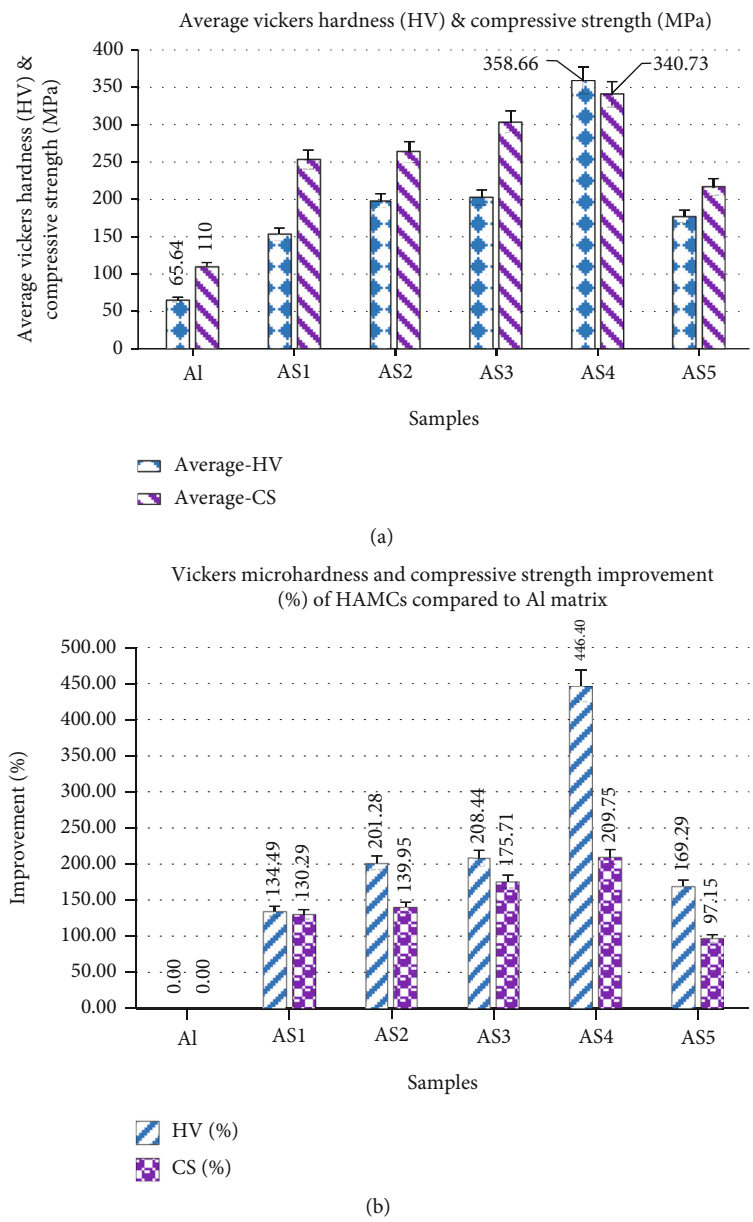

Figure 11: (a) Graph of average HV and CS values of HAMC samples; (b) improvement (%).

Table 11: Three trials and average CS values of the sintered HAMCs.

Sample	Chemical composition	CS_1	CS_2	CS_3	Average CS
Al	Pure Al metal	110.00	108.00	112.00	110.00
AS_1	$Al/5SiC/5Al_2O_3$	262.38	245.03	252.56	253.32
AS_2	$Al/5SiC/5Al_2O_3/0.5Gr/0.5SCBA$	273.00	255.65	263.18	263.94
AS_3	$Al/5SiC/5Al_2O_3/2.5Gr/2.5SCBA$	312.34	294.99	302.52	303.28
AS_4	$Al/5SiC/5Al_2O_3/4.5Gr/4.5SCBA$	349.78	332.44	339.96	340.73
AS_5	$Al/5SiC/5Al_2O_3/6.5Gr/6.5SCBA$	225.92	208.58	216.10	216.87

(iv) Compared to pure Al and double-reinforced AMCs, the newly synthesized tetra hybrid reinforced HAMCs demonstrated superior physicomechanical properties

(v) As a result, the developed HAMC material with lightweight, high strength, and low cost might have prospective applications in automobiles and

transportation, aerospace and defense, medical devices, wind power components, and structural applications

(vi) To reduce raw material costs, improve properties, and keep the environment clean, it is recommended to use various solid waste materials (rice husk ash, filter cake, corn cob ash, and others) and solid lubricants (MoS_2, Gr) as secondary reinforcements in HAMCs with various matrix materials. Secondary processes such as forging and extrusion are also recommended in HAMC synthesis to reduce porosity and increase tolerability

(vii) It is also highly recommended to use these materials in the form of nanosized particles as primary or secondary reinforcements to improve the material behavior of hybrid composites

Data Availability

The experimental data used to support the findings discussed in this study are included within the article.

Conflicts of Interest

The authors declare that they have no known competing financial interests or personal relationships that could have appeared to influence the work reported in this paper.

References

[1] D. K. Koli, G. Agnihotri, and R. Purohit, "Advanced aluminium matrix composites: the critical need of automotive and aerospace engineering fields," *Materials Today: Proceedings*, vol. 2, no. 4, pp. 3032–3041, 2015.

[2] M. Asif, K. Chandra, and P. Misra, "Development of aluminium based hybrid metal matrix composites for heavy duty applications," *Journal of Minerals and Materials Characterization and Engineering*, vol. 10, no. 14, pp. 1337–1344, 2011.

[3] A. Srivastava, P. Garg, A. Kumar, Y. Krishna, and K. K. Varshney, "A review on fabrication & characterization of hybrid aluminium metal matrix composite," *International Journal of Advance Research and Innovation*, vol. 2, pp. 242–246, 2014.

[4] P. Dev Srivyas and M. S. Charoo, "Application of hybrid aluminum matrix composite in automotive industry," *Materials Today: Proceedings*, vol. 18, pp. 3189–3200, 2019.

[5] S. Dhanesh, K. S. Kumar, L. Yohannan, N. K. M. Fayiz, and E. Sajith, "Aluminium metal matrix composites reinforced with non - conventional materials: a review," *Materials Today: Proceedings*, vol. 45, pp. 1371–1375, 2021.

[6] M. A. Fentahun and M. A. Sava, "Materials used in automotive manufacture and material selection using Ashby charts," *International Journal of Materials Engineering*, vol. 8, pp. 40–54, 2018.

[7] P. L. Menezes, C. J. Reeves, P. K. Rohatgi, and M. R. Lovell, "Self-lubricating behavior of graphite-reinforced composites," in *Tribology for Scientists and Engineers*, P. Menezes, M. Nosonovsky, S. Ingole, S. Kailas, and M. Lovell, Eds., pp. 341–389, Springer, New York: New York, 2013.

[8] A. Parveen, N. R. Chauhan, and M. Suhaib, "Influence of process parameters and reinforcements on aluminum hybrid composites developed by powder metallurgy process," *Physics of Metals and Metallography*, vol. 122, no. 10, pp. 1007–1013, 2021.

[9] D. M. Shinde, P. Sahoo, and J. P. Davim, "Tribological characterization of particulate-reinforced aluminum metal matrix nanocomposites: a review," *Advanced Composites Letters*, vol. 29, 2020.

[10] R. Chandel, N. Sharma, and S. A. Bansal, "A Review on Recent Developments of Aluminum-Based Hybrid Composites for Automotive Applications," *Emergent Materials*, vol. 4, no. 5, pp. 1243–1257, 2021.

[11] A. K. Srivastava, A. R. Dixit, and S. Tiwari, "A review on the intensification of metal matrix composites and its non-conventional machining," *Science and Engineering of Composite Materials*, vol. 25, no. 2, pp. 213–228, 2018.

[12] J. Chandradass, T. Thirugnanasambandham, P. Jawahar, and T. T. M. Kannan, "Effect of silicon carbide and silicon carbide/alumina reinforced aluminum alloy (AA6061) metal matrix composite," *Materials Today: Proceedings*, vol. 45, pp. 7147–7150, 2021.

[13] A. V. Muley, S. Aravindan, and I. P. Singh, "Nano and hybrid aluminum based metal matrix composites: an overview," *Manufacturing Review*, vol. 2, p. 15, 2015.

[14] P. Sharma, D. Khanduja, and S. Sharma, "Tribological and mechanical behavior of particulate aluminum matrix composites," *Journal of Reinforced Plastics and Composites*, vol. 33, no. 23, pp. 2192–2202, 2014.

[15] M. V. Krishna and A. M. Xavior, "An investigation on the mechanical properties of hybrid metal matrix composites," *Procedia Engineering*, vol. 97, pp. 918–924, 2014.

[16] T. Lokesh and U. S. Mallik, "Dry sliding wear behavior of Al/Gr/SiC hybrid metal matrix composites by Taguchi techniques," *Materials Today: Proceedings*, vol. 4, no. 10, pp. 11175–11180, 2017.

[17] B. Hadzima and D. Arsic, "Influence of load and reinforcement content on selected tribological properties of Al/SiC/Gr hybrid composites," *Production Engineering Archives*, vol. 18, no. 18, pp. 18–23, 2018.

[18] I. Manivannan, S. Ranganathan, S. Gopalakannan, and S. Suresh, "Mechanical properties and tribological behavior of Al6061–SiC–Gr self-lubricating hybrid nanocomposites," *Transactions of the Indian Institute of Metals*, vol. 71, no. 8, pp. 1897–1911, 2018.

[19] J. Singh, "Fabrication characteristics and tribological behavior of Al/SiC/Gr hybrid aluminum matrix composites: a review," *Friction*, vol. 4, no. 3, pp. 191–207, 2016.

[20] S. Veličković Gajević, S. Miladinović, B. Stojanović et al., "Tribological characteristics of Al/SiC/Gr hybrid composites," *MATEC Web of Conferences*, vol. 183, article 02001, 2018.

[21] M. O. Bodunrin, K. K. Alaneme, and L. H. Chown, "Aluminium matrix hybrid composites: a review of reinforcement philosophies; mechanical, corrosion and tribological characteristics," *Journal of Materials Research and Technology*, vol. 4, no. 4, pp. 434–445, 2015.

[22] J. Singh and A. Chauhan, "A review on sliding wear behaviour of aluminium matrix composites with hybrid reinforcements for automotive applications," *Tribology Online*, vol. 9, no. 3, pp. 121–134, 2014.

[23] G. Arora and S. Sharma, "A review on monolithic and hybrid metal–matrix composites reinforced with industrial-

agro wastes," *Journal of the Brazilian Society of Mechanical Sciences and Engineering*, vol. 39, no. 11, pp. 4819–4835, 2017.

[24] P. P. Kulkarni, B. Siddeswarappa, and K. S. H. Kumar, "A survey on effect of agro waste ash as reinforcement on aluminium base metal matrix composites," *Open Journal of Composite Materials*, vol. 9, no. 3, pp. 312–326, 2019.

[25] K. M. Singh and A. K. Chauhan, "Fabrication, characterization, and impact of heat treatment on sliding Wear behaviour of aluminium metal matrix composites reinforced with B_4C," *Advances in Materials Science and Engineering*, vol. 2021, Article ID 5554837, 9 pages, 2021.

[26] D. B. Miracle, "Metal matrix composites–from science to technological significance," *Composites Science and Technology*, vol. 65, no. 15-16, pp. 2526–2540, 2005.

[27] N. Miloradović, R. Vujanac, and A. Pavlović, "Wear behaviour of ZA27/SiC/graphite composites under lubricated sliding conditions," *Materials*, vol. 13, no. 17, article 3752, 2020.

[28] M. Guttikonda, K. Pandey, and S. Maity, "Effect of Variations in Microwave Processing Temperatures on Microstructural and Mechanical Properties of AA7075/SiC/Graphite Hybrid Composite Fabricated by Powder Metallurgy Techniques," *Silicon*, 2022.

[29] N. Dawoud, A. Micheal, and R. R. Moussa, "A review on investigating the experimental process for partial replacement of cement with sugarcane bagasse in the construction industry," *IOP Conference Series: Materials Science and Engineering*, vol. 974, no. 1, article 012036, 2020.

[30] M. Sultana and A. Rahman, "Characterization of Calcined Sugarcane Bagasse Ash and Sugarcane Waste Ash for Industrial Use," in *International Conference on Mechanical, Industrial and Materials Engineering 2013 (ICMIME2013)*, Rajshahi, Bangladesh, 2013.

[31] I. A. Ibrahim, F. A. Mohamed, and E. J. Lavernia, "Particulate reinforced metal matrix composites—a review," *Journal of Materials Science*, vol. 26, no. 5, pp. 1137–1156, 1991.

[32] M. K. Surappa, "Aluminium matrix composites: challenges and opportunities," *Sadhana*, vol. 28, no. 1-2, pp. 319–334, 2003.

[33] J. W. Kaczmar, K. Pietrzak, and W. Włosiński, "The production and application of metal matrix composite materials," *Journal of Materials Processing Technology*, vol. 106, no. 1-3, pp. 58–67, 2000.

[34] K. K. Chawla, "Metal matrix composites," in *Composite Materials*, pp. 197–248, Springer, New York, NY, 2012.

[35] D. J. Lloyd, "Particle reinforced aluminium and magnesium matrix composites," *International Materials Reviews*, vol. 39, no. 1, pp. 1–23, 1994.

[36] W. Yemane, *Design, Development and Performance Evaluation of a Diesel Engine Driven Mechanical Sugarcane Harvester*, Adama Science and Technology University, 2020.

[37] N. K. Bhoi, H. Singh, and S. Pratap, "Developments in the aluminum metal matrix composites reinforced by micro/nano particles–a review," *Journal of Composite Materials*, vol. 54, no. 6, pp. 813–833, 2020.

[38] S. M. Mahdi and L. Ghalib, "Corrosion behavior of Al/SiC composite prepared by powder metallurgy in chloride environments," *Journal of Bio- and Tribo-Corrosion*, vol. 8, no. 1, p. 8, 2021.

[39] Y. B. Liu, S. C. Lim, L. Lu, and M. O. Lai, "Recent development in the fabrication of metal matrix-particulate composites using powder metallurgy techniques," *Journal of Materials Science*, vol. 29, no. 8, pp. 1999–2007, 1994.

[40] A. Mussatto, I. U. I. Ahad, R. T. Mousavian, Y. Delaure, and D. Brabazon, "Advanced production routes for metal matrix composites," *Engineering Reports*, vol. 3, no. 5, 2021.

[41] A. A. Mazen and A. Y. Ahmed, "Mechanical behavior of Al-Al_2O_3 MMC manufactured by PM techniques part I—scheme I processing parameters," *Journal of Materials Engineering and Performance*, vol. 7, no. 3, pp. 393–401, 1998.

[42] A. Dubey, P. Khosla, H. K. Singh, V. Katoch, D. Kumar, and P. Gupta, "A review on role of processing parameter in determining properties of silicon carbide reinforced metal matrix nanocomposites," *Journal of Applied Science and Engineering*, vol. 19, no. 3, pp. 303–312, 2016.

[43] M. Z. Hussain, S. Khan, R. Nagarajan, U. Khan, and V. Vats, "Fabrication and microhardness analysis of MWCNT/MnO2 nanocomposite," *Journal of Materials*, vol. 2016, Article ID 6070468, 10 pages, 2016.

[44] A. Bahrami, N. Soltani, M. I. Pech-Canul, and C. A. Gutiérrez, "Development of metal-matrix composites from industrial/agricultural waste materials and their derivatives," *Critical Reviews in Environmental Science and Technology*, vol. 46, no. 2, pp. 143–208, 2016.

[45] G. F. Aynalem, "Processing methods and mechanical properties of aluminium matrix composites," *Advances in Materials Science and Engineering*, vol. 2020, Article ID 3765791, 19 pages, 2020.

[46] M. A. Alam, H. H. Ya, M. Yusuf et al., "Modeling, Optimization and performance evaluation of TiC/graphite reinforced Al 7075 hybrid composites using response surface methodology," *Materials*, vol. 14, no. 16, article 4703, 2021.

[47] P. Ravindran, K. Manisekar, S. Vinoth Kumar, and P. Rathika, "Investigation of microstructure and mechanical properties of aluminum hybrid nano-composites with the additions of solid lubricant," *Materials & Design*, vol. 51, pp. 448–456, 2013.

[48] S. Suresha and B. K. Sridhara, "Friction characteristics of aluminium silicon carbide graphite hybrid composites," *Materials & Design*, vol. 34, pp. 576–583, 2012.

[49] P. P. Ikubanni, M. Oki, A. A. Adeleke, and P. O. Omoniyi, "Synthesis, physico-mechanical and microstructural characterization of Al6063/SiC/PKSA hybrid reinforced composites," *Scientific Reports*, vol. 11, no. 1, article 14845, 2021.

[50] V. S. S. Venkatesh and A. B. Deoghare, "Effect of sintering mechanisms on the mechanical behaviour of SiC and kaoline reinforced hybrid aluminium metal matrix composite fabricated through powder metallurgy technique," *Silicon*, vol. 14, no. 10, pp. 5481–5493, 2021.

[51] M. K. Gupta, P. K. Rakesh, and I. Singh, "Application of industrial waste in metal matrix composite," *Journal of Polymer & Composites*, vol. 4, no. 3, pp. 27–34, 2019.

[52] J. Fayomi, A. P. I. Popoola, and O. M. Popoola, "Corrosion performances and thermal behavior of AA8011 reinforced with hybrid-nano ZrB_2+ Si_3N_4 particulates for automobile applications," *Materials Research Express*, vol. 6, no. 11, p. 1150e2, 2019.

[53] N. Prabha and J. Dhas, "Effect of TiC and MOS_2 reinforced aluminium metal matrix composites on microstructure and thermogravimetric analysis," *Rasayan Journal of Chemistry*, vol. 10, pp. 729–737, 2017.

[54] S. Lal, S. Kumar, and Z. A. Khan, "Microstructure evaluation, thermal and mechanical characterization of hybrid metal

matrix composite," *Science and Engineering of Composite Materials*, vol. 25, no. 6, pp. 1187–1196, 2018.

[55] K. Park, D. Kim, K. Kim, S. Cho, and H. Kwon, "Behavior of intermetallic compounds of Al-Ti composite manufactured by spark plasma sintering," *Materials*, vol. 12, no. 2, p. 331, 2019.

[56] C. A. Leon-Patino, *Infiltration Processing of Metal Matrix Composites Using Coated Ceramic Particulates, [Ph. D thesis]*, McGill University, 2001.

[57] V. Singh, S. Chauhan, P. C. Gope, and A. K. Chaudhary, "Enhancement of wettability of aluminum based silicon carbide reinforced particulate metal matrix composite," *High Temperature Materials and Processes*, 2014.

[58] D. W. Wolla, M. J. Davidson, and A. K. Khanra, "Studies on the formability of powder metallurgical aluminum–copper composite," *Materials & Design*, vol. 59, pp. 151–159, 2014.

[59] Ankur, A. Bharti, D. Prasad, N. Kumar, and K. K. Saxena, "A re-investigation: effect of various parameter on mechanical properties of copper matrix composite fabricated by powder metallurgy," *Materials Today: Proceedings*, vol. 45, pp. 4595–4600, 2021.

[60] S. Kúdela, S. Oswald, S. Kúdela, and K. Wetzig, "Application of FTIR spectra for evaluating interfacial reactions in metal matrix composites," *Analytical and Bioanalytical Chemistry*, vol. 390, no. 6, pp. 1477–1486, 2008.

[61] H. S. Vaziri, A. Shokuhfar, and S. S. S. Afghahi, "Synthesis of WS2/CNT hybrid nanoparticles for fabrication of hybrid aluminum matrix nanocomposite," *Materials Research Express*, vol. 7, no. 2, article 025034, 2020.

[62] J. A. Gadsden, *Infrared Spectra of Minerals and Related Inorganic c Ompounds*, Adama Science and Technology University, 1975.

[63] M. Merabtene, L. Kacimi, and P. Clastres, "Elaboration of geopolymer binders from poor kaolin and dam sludge waste," *Heliyon*, vol. 5, no. 6, article e01938, 2019.

[64] V. Hospodarova, E. Singovszka, and N. Stevulova, "Characterization of cellulosic fibers by FTIR spectroscopy for their further implementation to building materials," *American Journal of Analytical Chemistry*, vol. 9, no. 6, pp. 303–310, 2018.

[65] L. Feng, Z. Yan, X. Shi, and F. Sultonzoda, "Anti-icing/frosting and self-cleaning performance of superhydrophobic aluminum alloys," *Applied Physics A*, vol. 124, no. 2, 2018.

[66] C830-00 A, *Standard test methods for apparent porosity, liquid absorption, apparent specific gravity, and bulk density of refractory shapes by vacuum pressure*, ASTM, 2016.

[67] S. Sahoo, S. Samal, and B. Bhoi, "Fabrication and characterization of novel Al-SiC-hBN self-lubricating hybrid composites," *Materials Today Communications*, vol. 25, article 101402, 2020.

[68] L. Jinfeng, J. Longtao, W. Gaohui, T. Shoufu, and C. Guoqin, "Effect of graphite particle reinforcement on dry sliding wear of SiC/Gr/Al composites," *Rare Metal Materials and Engineering*, vol. 38, no. 11, pp. 1894–1898, 2009.

[69] D. S. Prasad, C. Shoba, and N. Ramanaiah, "Investigations on mechanical properties of aluminum hybrid composites," *Journal of Materials Research and Technology*, vol. 3, no. 1, pp. 79–85, 2014.

[70] M. Singla, D. D. Dwivedi, L. Singh, and V. Chawla, "Development of aluminium based silicon carbide particulate metal matrix composite," *Journal of Minerals and Materials Characterization and Engineering*, vol. 8, no. 6, pp. 455–467, 2009.

[71] E. W. Fanani, E. Surojo, A. R. Prabowo, and H. I. Akbar, "Recent progress in hybrid aluminum composite: manufacturing and application," *Metals*, vol. 11, no. 12, article 1919, 2021.

[72] N. Radhika, R. Subramanian, S. Venkat Prasat, and B. Anandavel, "Dry sliding wear behaviour of aluminium/alumina/graphite hybrid metal matrix composites," *Industrial Lubrication and Tribology*, vol. 64, no. 6, pp. 359–366, 2012.

[73] N. Radhika and R. Subramaniam, "Wear Behaviour of Aluminium/Alumina/Graphite Hybrid Metal Matrix Composites Using Taguchi's Techniques," *Industrial Lubrication and Tribology*, vol. 65, no. 3, pp. 166–174, 2013.

[74] M. G. Madhu, H. K. Shivanand, P. Maibusab, and R. Kiran, "Investigations on Mechanical Properties of Heat-Treated Aluminum 7075/Graphite Powder/Bagasse Ash Hybrid Metal Matrix Composites," *International Journal of Scientific Research in Science, Engineering and Technology*, 2019.

[75] M. K. Sahu and R. K. Sahu, "Experimental investigation, modeling, and optimization of wear parameters of B4C and fly-ash reinforced aluminum hybrid composite," *Frontiers in Physics*, vol. 8, 2020.